Journal of Power Sources 233 (2013) 341–345

Contents lists available at SciVerse ScienceDirect

Journal of Power Sources

journal homepage: www.elsevier.com/locate/jpowsour

Short communication

In search of high performance anode materials for Mg batteries: Computational studies of Mg in Ge, Si, and Sn

Oleksandr I. Malyi [a,*], Teck L. Tan [b], Sergei Manzhos [a,*]

[a] Department of Mechanical Engineering, National University of Singapore, Block EA #07-08, 9 Engineering Drive 1, Singapore 117576, Singapore
[b] Institute of High Performance Computing, 1 Fusionopolis Way, #16-16 Connexis, Singapore 138632, Singapore

HIGHLIGHTS

- Prospective anode materials for Mg batteries studied ab initio.
- Mg diffusion, voltages, volume expansion studied in Si, Ge, Sn.
- Mg–Mg interactions decrease diffusion barrier.
- Highest Mg capacity, largest volume expansion in Si.
- Lower volume expansion, lower diffusion barriers in Ge, Sn.

GRAPHICAL ABSTRACT

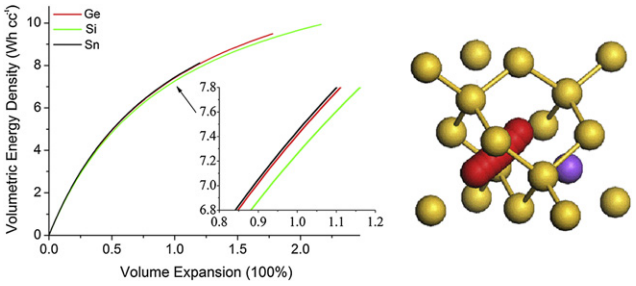

ARTICLE INFO

Article history:
Received 21 December 2012
Received in revised form
15 January 2013
Accepted 19 January 2013
Available online 29 January 2013

Keywords:
Magnesium batteries
Anode
Density functional theory
Insertion
Diffusion
Voltages

ABSTRACT

We present ab initio studies of structures, energetics, and diffusion properties of Mg in bulk Si, Ge, and Sn diamond structures to evaluate their potential as insertion type anode materials for Mg batteries. We show that Si could provide the highest specific capacity (3817 mAh g^{-1}) and the lowest average insertion voltage (~0.15 eV vs. Mg) for Mg storage. Nevertheless, due to its significant percent lattice expansion (~216%) and slow Mg diffusion, Sn and Ge are more attractive; both anodes have lower lattice expansions (~120% and ~178%, respectively) and diffusion barriers (~0.50 and ~0.70 eV, respectively, for single-Mg diffusion) than Si. We show that Mg–Mg interactions at different stages of charging can decrease significantly the diffusion barrier compared to the single atom diffusion, by up to 0.55 eV.

1. Introduction

Increased needs in energy storage and limited access to Li resources lead to a shift of interest to non-Li ion batteries. Metals such as Na [1–3], Mg [4,5], Al [6] are attractive for energy storage applications because of their low cost and availability. While Na batteries are attractive and in fact used [1] for bulk storage, they are not very suitable for applications where high energy density is required, such as all-electric vehicles and portable electronics, due to the low rate capability and specific capacity of Na storage electrodes [2,3]. The research into the potential of batteries using other metals such as Ca [7] or Al [6] is still in its infancy. Mg batteries, on the other hand, are currently emerging as a viable next generation rechargeable battery technology, so much so that commercialization is believed to be achievable with several companies working on it [4,5,8]. The key advantages of Mg include: (i) it results in the storage of up to 2 electrons per Mg atom vs. one for Li and Na, resulting in a higher theoretical volumetric energy density and a specific capacity comparable to those of Li in spite of being heavier

* Corresponding authors. Tel.: +65 6516 4605; fax: +65 6779 1459.
E-mail address: mpemanzh@nus.edu.sg (S. Manzhos).

0378-7753/$ – see front matter © 2013 Elsevier B.V. All rights reserved.
http://dx.doi.org/10.1016/j.jpowsour.2013.01.114

than both Li and Na; (ii) metallic Mg is cheaper than metallic Li; (iii) the atomic radius of Mg is smaller than that of Na and is comparable to Li. A smaller size is expected to result in higher diffusion rates and therefore a better battery rate capability, and (iv) Mg does not have a severe dendrite formation problem that plagues metallic Li and Na [9,10]. In fact, most works on Mg batteries [8,11,12] used metallic Mg anodes and focused on the development of cathode materials. The cycling ability of Mg batteries, however, remained poor. This has in particular to do with reactions of the anode with electrolyte species resulting in the formation of a blocking layer [8]. Electrode–electrolyte interactions also limit the achievable battery voltage. High voltage Mg batteries can be developed if the metallic anode is replaced with an insertion anode [4,5]. *Simply put, the success of Mg batteries may depend on successful design of Mg anodes*. Insertion type anode materials have been extensively researched for Li batteries. Specifically, group IV elements (Ge, Si, and Sn) have been shown to result in very high Li specific capacities (up to 4400 mAh g^{-1} (Si)). The possibilities of insertion anodes in Mg batteries are still largely unstudied. There have been recent and encouraging experimentations with insertion anodes. Singh et al. [4,5] have reported investigations of Mg batteries with Sb, Sn, and Bi anodes. Theoretical studies of Mg insertion anodes are, however, lacking but are critical to guide the design of new electrode materials. The performance of the anode material is heavily dependent on the type of metal atom: qualitative differences in insertion structures and in voltage profiles have been reported [2,4,5,13]. Differences in diffusion properties can potentially result in drastic differences in battery rate capabilities for different metal ions. In this study, we analyze the potential of Ge, Si, and Sn for bulk storage and the high energy density applications. Based on density functional theory (DFT) calculations (see Supporting Information), we study structures, energetics, and diffusion properties of Mg in Si, Ge, and Sn, including the effects on the diffusion barrier of Mg–Mg interactions and of high anode charge states–alloys XMg_2, where X = Ge, Si, and Sn. Although β-X structures can be more stable under some conditions, here, we focus on diamond like structures (α-X) as potential anode materials.

2. Results and discussion

It has been reported that at high dopant concentrations, Mg interacts with X forming XMg_2 (Fm3m space group) structures and that for a wide range of Mg concentrations, X coexists with XMg_2 structures [14]. Among the considered materials, Si can provide the highest specific capacity (see Table 1). For instance, the theoretical specific capacity for Si is 2906 mAh g^{-1} and 2341 mAh g^{-1} larger than those of Sn and Ge, respectively. Taking into account that Li and Mg have one and two valence electrons, respectively, and using the methodology proposed by Ceder et al. [15], the average insertion voltage (V) vs. metallic Mg for the prospective anode materials is predicted using Eq. (1):

$$V = -\frac{E(XMg_2) - E(X) - 2E(Mg)}{4e}, \quad (1)$$

where E is the total energy of the reference state (see Table S1) as calculated using DFT, e is the absolute value of the electron charge.

Table 1
Specific capacity (mAh g^{-1}), percent volume expansion (%) at full state of charge, and voltage (V) for $GeMg_2$, $SiMg_2$, and $SnMg_2$.

Element	Specific capacity	Volume expansion	Voltage
Ge	1476	178	0.241
Si	3817	216	0.151
Sn	911	120	0.184

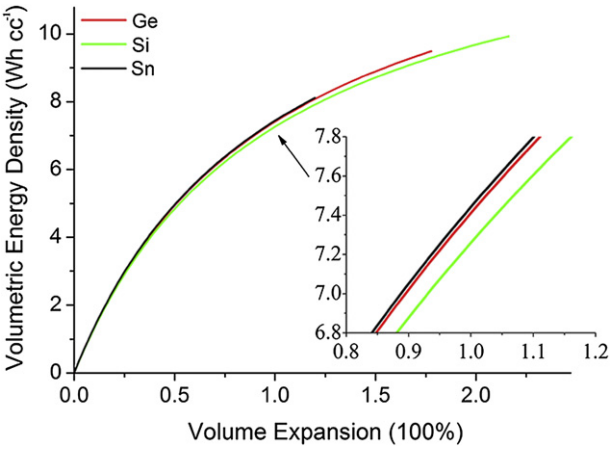

Fig. 1. Volumetric energy density for Mg–X alloys as a function of volume expansion.

The lowest average voltage (0.151 V) is found for $SiMg_2$ (see Table 1), while for $GeMg_2$, the largest voltage (0.241 V) is predicted. Although both the specific capacity and the average insertion voltage are important for the performance of metal ion batteries, an insertion type anode can also have a significant expansion during charging/discharging process. Anode materials having low average insertion voltages and high specific capacities but huge lattice expansions may not be appropriate for specific battery applications. This is because a significant anode deformation changes its mechanical stability [16] and consequently can adversely affect the battery's cyclability. This problem is well known for the Si anode in Li batteries and its resolution required transition to nanostructured materials [17], which also results in capacities much lower than theoretical [18–20] as well as in an increased cost. Therefore, starting with a material having a smaller expansion as well as a high capacity and suitable voltages would clearly be advantageous.

To evaluate prospective anode materials, Obrovac et al. [13] predicted not only voltages and specific capacities but also volumetric energy densities (Wh cc^{-1}) and the extent of the materials' expansion. Using the same methodology, the volumetric energy density ($\tilde{U}_f$) of a charged negative electrode alloy material can be calculated according to Eq. (2):

$$\tilde{U}_f = \frac{FV_{avg}}{\nu}\left(\frac{\xi_f}{1+\xi_f}\right), \quad (2)$$

where F is Faraday's constant (26.802 Ah mol^{-1}); ξ_f is the final percent volume expansion (in a fully charged anode material); V_{avg} is the average voltage of the alloy vs. a cathode; ν is the volume

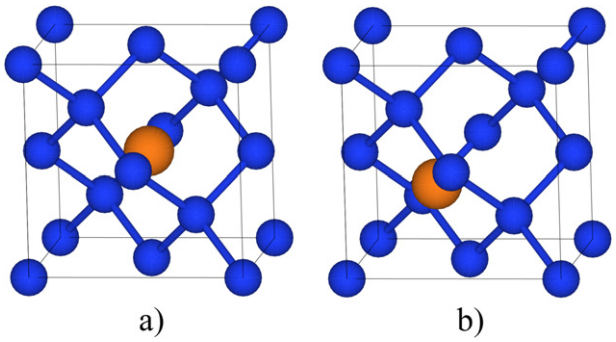

Fig. 2. Tetragonal (a) and hexagonal (b) insertion sites in Ge, Si, and Sn (=X). Orange – Mg atoms, blue – X atoms. (For interpretation of the references to color in this figure legend, the reader is referred to the web version of this article.)

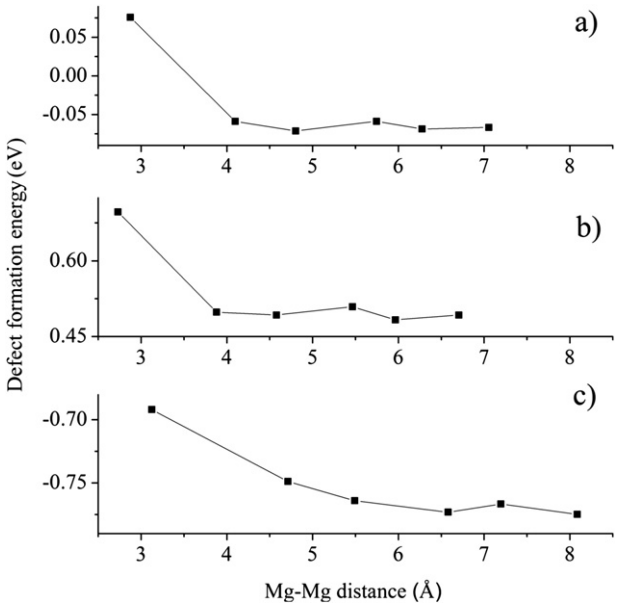

Fig. 3. Formation energies of Mg–Mg defects as functions of Mg–Mg distance in Ge (a), Si (b), and Sn (c).

occupied by Mg, per valence electron [21]. Since in the recent studies, volumetric energy densities were predicted vs. a 3.75 V cathode, we also used that value for the reference state of cathode. Predicted volumetric energy densities show much smaller differences between the three anode materials than the differences of specific capacities and average voltages. Si can provide the largest volumetric energy density (9.929 Wh cc^{-1}) at a ~216% volume expansion; while Ge can provide 9.487 Wh cc^{-1} at ~178%, as shown in Fig. 1. Fig. 1 has practical significance for the design of anodes. For example, suppose one is able to design an X-based anode that withstands a 100% volume expansion, then the volumetric energy density can be predicted according to the figure. In this light, it is important to consider volumetric energy densities for the prospective anode materials at the same volume expansion. For a 100% volume expansion, Sn and Ge can provide almost the same volumetric energy densities (7.413 Wh cc^{-1} and 7.382 Wh cc^{-1}, respectively) which are ~0.151 Wh cc^{-1} larger than that of Si (7.231 Wh cc^{-1}). It should be noted that recently Obrovac et al. [21] predicted volumetric energy densities for β-Sn. They found that Si has the volumetric energy density larger by ~1.377 Wh cc^{-1} compared to that of β-Sn. The difference between our and that prediction is explained by a different Mg volume occupied in α-Sn (6.42 mL mol^{-1} $charge^{-1}$) and β-Sn (7.57 mL mol^{-1} $charge^{-1}$) [21]. Taking into account that α-Sn/β-Sn phase transition takes place at ~287 K and can be changed by doping [22], environmental conditions [23,24] etc., it becomes clear that the use of stabilized α-Sn can provide a much better performance compared to that of β-Sn.

All three materials can take up to 2 Mg atoms per host atom, and therefore, for a realistic comparison of their rate capabilities, it is critical to investigate the diffusion behavior of Mg atoms at different concentrations. For low concentrations, the computed defect formation energies (see Table S2) suggest that Mg atoms in all three prospective anode materials act as interstitial defects occupying tetragonal (T) sites (see Fig. 2(a)). This is similar to the behavior of Li [25] and Na [26] atoms in the Si matrix. Addition of a second Mg atom leads to the Mg–Mg interaction changing the stability of Mg defects. The predicted formation energies of Mg–Mg defects suggest that Mg atoms do not tend to cluster (see Fig. 3). At low dopant concentrations, the insertion process is associated with migration of Mg atoms from one T site to another. Our calculations suggest that for all considered structures, the Mg atom migrates between two T sites via a hexagonal (Hex) site (see Fig. 2(b)). Despite this similarity, Mg diffusion barriers are very different for the three systems (see Fig. 4(a)). The lowest Mg migration barrier (0.497 eV) is predicted for Sn and it is 0.503 eV smaller than that for Si. This observation suggests that the initial stage of Mg insertion is significantly faster for Sn compared to the other materials. As a second Mg atom comes into the matrix, Mg–Mg interactions change Mg diffusion behavior. Specifically, when two Mg atoms are close to each other, the predicted migration barriers are smaller compared to those for single Mg atoms (see Fig. 4(b)). This is caused by both a local expansion of the matrix and a destabilizing effect of Mg–Mg interactions (see Fig. 3). Indeed, a local expansion caused by deformation or additional atoms can reduce the migration barrier [26]. Hence, Mg–Mg interaction can increase Mg diffusivity for some range of doping concentrations. Nevertheless, due to a large energy cost of clustering, it is expected to be less likely compared to both Li and Na [26] at the concentrations considered here.

The increase of Mg concentration eventually leads to the formation of bulk XMg_2 structures or coexistence of XMg_2 and X structures. The diffusion behavior of Mg atoms can then be described as diffusion in defected bulk XMg_2 structures. Ionic conductivity of such compound strongly depends on the Mg vacancy concentration. In the simplest case, for an almost fully charged anode, it can be analyzed as the diffusion of a lone Mg

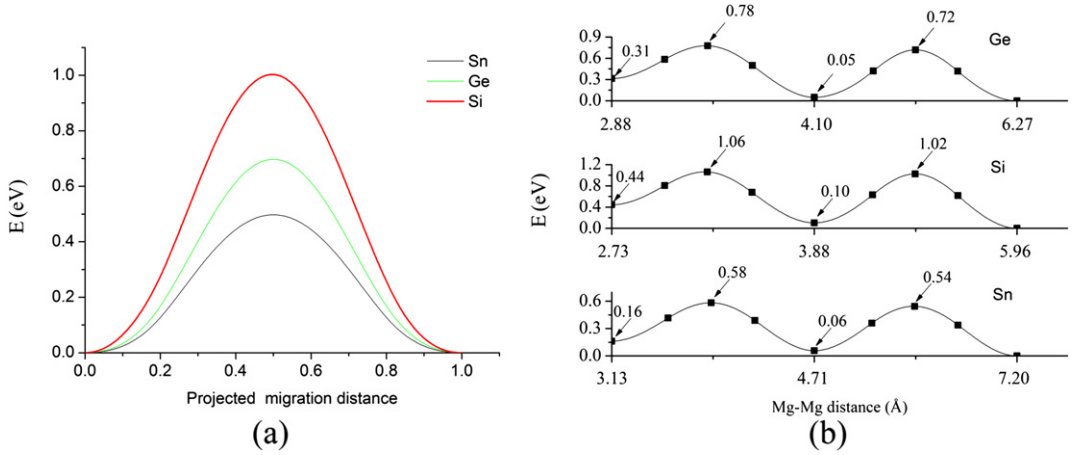

Fig. 4. (a) Migration barriers for diffusion of a Mg atom between two tetragonal sites of Ge, Si, and Sn. (b) The migration barriers of Mg in bulk Ge, Si, and Sn vs. Mg–Mg distance in the bulk materials.

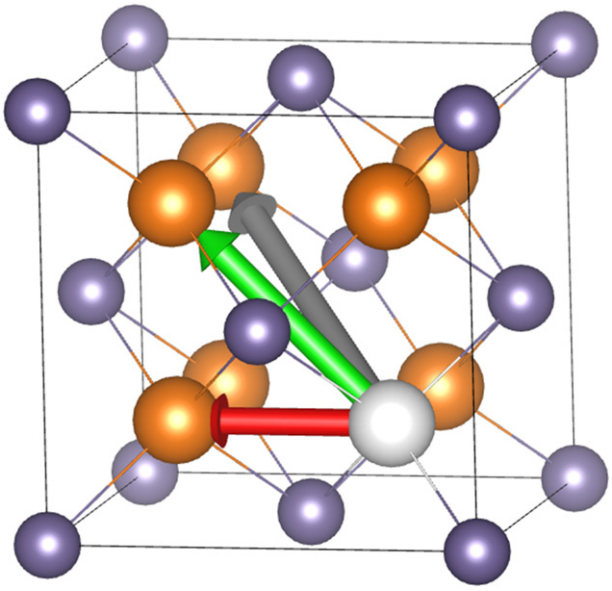

Fig. 5. Possible migration pathways for a Mg (vacancy) atom in XMg_2 structures (X = Ge, Si, Sn). Red, green, and gray colors represent [100], [110], and [110] directions for vacancy migrations. Orange – Mg atoms, gray – Mg vacancy, blue – X atoms. (For interpretation of the references to color in this figure legend, the reader is referred to the web version of this article.)

vacancy (Mg atom) between two tetragonal positions (see Fig. S1) in XMg_2 structures. This still provides a general understanding of diffusion properties in prospective anode materials at high states of charge. For systems with a single Mg vacancy in an XMg_2 structure, three different migration pathways exist (see Fig. 5). Similar to investigations of oxygen diffusion in cubic zirconia [27] and ceria [28], we find that the lowest migration barrier corresponds to Mg migration along the [100] direction. For other migration pathways, cation–cation interactions significantly increase (by more than 0.5 eV) the migration barriers (see Table 2). Mg diffusion in XMg_2 structures can thus be described as motion of a Mg atom between two nearest Mg sites and the contributions from other pathways can be ignored. These results suggest that for XMg_2 with the same concentrations of Mg vacancies, Ge based materials should have the highest ionic conductivity among the considered XMg_2 structures.

Since the charging/discharging rate is more important than the volumetric energy density for bulk storage applications [29], the trend in diffusion barriers among the 3 materials at different Mg concentrations computed here is of practical significance for electrode design. For instance, the low Mg diffusivity of Si suggests that its use as an anode material for bulk storage Mg-ion batteries is questionable. It is also expected that, due to the possible existence of inhomogeneous structures during metal insertion and high Mg diffusion barriers in Mg-poor structures, it may be difficult to achieve the maximum theoretic volumetric energy density for Si based materials. In contrast, both Ge and Sn, having low Mg diffusion barriers (comparable with migration barrier of Li atoms in Si (0.61 eV) [26]) for a range of dopant concentrations, are attractive anode materials for both high volumetric energy density and bulk storage applications.

Table 2
Migration barriers (in eV) of single Mg vacancy in XMg_2 structures.

	[100]	[110]	[111]
$GeMg_2$	0.419	1.378	1.418
$SiMg_2$	0.444	1.438	1.475
$SnMg_2$	0.497	0.948	0.955

3. Conclusions

In summary, based on DFT calculations, we have investigated the potential of bulk α-X (X = Ge, Si, and Sn) systems as anode materials for Mg batteries. We find that all considered materials can provide comparable capacities and larger volumetric energy densities compared to those for Li batteries. The results show that Sn could provide the largest volumetric energy density (7.413 Wh cc^{-1}) at a 100% volume expansion and the lowest migration barrier for the diffusion of a single Mg atom (0.497 eV). Hence, using stabilized diamond Sn can provide the best performance among the considered materials. A slightly weaker performance can be observed for the Ge anode, which can provide a comparable volumetric energy density (7.382 Wh cc^{-1}) and slightly larger migration barriers for low dopant concentrations. Hence, Ge and Sn based materials can be attractive anode materials for both high volumetric energy density and bulk storage applications. As the concentration of Mg atoms increases, Mg–Mg interactions are expected to drive down the diffusion barrier by as much as 0.38 eV, a similar effect to that predicted by us for Li and Na diffusion in Si [26]. The barrier in the XMg_2 phase is also much lower than that at the beginning of the charging process. Therefore, while most theoretical studies of diffusion in battery electrode materials were done for a single dopant atom or ion [30,31], we clearly demonstrate that the inclusion of metal–metal interactions is required for a realistic computational analysis of electrode materials.

Acknowledgments

This work was supported by the Tier 1 AcRF Grant by the Ministry of Education of Singapore (R-265-000-430-133). We gratefully acknowledge the use of supercomputers in A-STAR Computational Resource Centre (ACRC) and support from the Institute of High Performance Computing of A-STAR Singapore.

Appendix A. Supporting information

Supporting information related to this article can be found at http://dx.doi.org/10.1016/j.jpowsour.2013.01.114.

References

[1] V. Palomares, P. Serras, I. Villaluenga, K.B. Hueso, J. Carretero-Gonzalez, T. Rojo, Energy Environ. Sci. 5 (2012) 5884–5901.
[2] V.L. Chevrier, G. Ceder, J. Electrochem. Soc. 158 (2011) A1011–A1014.
[3] S.W. Kim, D.H. Seo, X.H. Ma, G. Ceder, K. Kang, Adv. Energy Mater. 2 (2012) 710–721.
[4] T.S. Arthur, N. Singh, M. Matsui, Electrochem. Commun. 16 (2012) 103–106.
[5] N. Singh, T.S. Arthur, C. Ling, M. Matsui, F. Mizuno, Chem. Commun. 49 (2013) 149–151.
[6] S. Liu, J.J. Hu, N.F. Yan, G.L. Pan, G.R. Li, X.P. Gao, Energy Environ. Sci. 5 (2012) 9743–9746.
[7] M. Hayashi, H. Arai, H. Ohtsuka, Y. Sakurai, J. Power Sources 119–121 (2003) 617–620.
[8] D. Aurbach, Z. Lu, A. Schechter, Y. Gofer, H. Gizbar, R. Turgeman, Y. Cohen, M. Moshkovich, E. Levi, Nature 407 (2000) 724–727.
[9] D. Aurbach, I. Weissman, Y. Gofer, E. Levi, Chem. Rec. 3 (2003) 61–73.
[10] J.O. Besenhard, M. Winter, ChemPhysChem 3 (2002) 155–159.
[11] T. Ichitsubo, T. Adachi, S. Yagi, T. Doi, J. Mater. Chem. 21 (2011) 11764–11772.
[12] R. Zhang, X. Yu, K.-W. Nam, C. Ling, T.S. Arthur, W. Song, A.M. Knapp, S.N. Ehrlich, X.-Q. Yang, M. Matsui, Electrochem. Commun. 23 (2012) 110–113.
[13] M.N. Obrovac, L. Christensen, D.B. Le, J.R. Dahnb, J. Electrochem. Soc. 154 (2007) A849–A855.
[14] I.-H. Jung, J. Kim, J. Alloys Compd. 494 (2010) 137–147.
[15] M.K. Aydinol, A.F. Kohan, G. Ceder, K. Cho, J. Joannopoulos, Phys. Rev. B 56 (1997) 1354–1365.

[16] M. Mortazavi, J. Deng, V.B. Shenoy, N.V. Medhekar, J. Power Sources 225 (2013) 207–214.
[17] H. Wu, Y. Cui, Nano Today 7 (2012) 414–429.
[18] M.Y. Ge, J.P. Rong, X. Fang, C.W. Zhou, Nano Lett. 12 (2012) 2318–2323.
[19] H. Wu, G. Zheng, N. Liu, T.J. Carney, Y. Yang, Y. Cui, Nano Lett. 12 (2012) 904–909.
[20] N. Liu, H. Wu, M.T. McDowell, Y. Yao, C. Wang, Y. Cui, Nano Lett. 12 (2012) 3315–3321.
[21] T.T. Tran, M.N. Obrovac, J. Electrochem. Soc. 158 (2011) A1411–A1416.
[22] E.A. Fitzgerald, P.E. Freeland, M.T. Asom, W.P. Lowe, R.A. Macharrie, B.E. Weir, A.R. Kortan, F.A. Thiel, Y.H. Xie, A.M. Sergent, S.L. Cooper, G.A. Thomas, L.C. Kimerling, J. Electron. Mater. 20 (1991) 489–501.
[23] J.Z. Hu, I.L. Spain, Solid State Commun. 51 (1984) 263–266.
[24] N.E. Christensen, M. Methfessel, Phys. Rev. B 48 (1993) 5797–5807.
[25] W.H. Wan, Q.F. Zhang, Y. Cui, E.G. Wang, J. Phys. Condens. Matter 22 (2010) 415501.
[26] O.I. Malyi, T.L. Tan, S. Manzhos, Appl. Phys. Express 6 (2013) 027301.
[27] O.I. Malyi, P. Wu, V.V. Kulish, K. Bai, Z. Chen, Solid State Ionics 212 (2012) 117–122.
[28] M. Nakayama, M. Martin, Phys. Chem. Chem. Phys. 11 (2009) 3241–3249.
[29] E. Barbour, I.A.G. Wilson, I.G. Bryden, P.G. McGregor, P.A. Mulheran, P.J. Hall, Energy Environ. Sci. 5 (2012) 5425–5436.
[30] Q.F. Zhang, W.X. Zhang, W.H. Wan, Y. Cui, E.G. Wang, Nano Lett. 10 (2010) 3243–3249.
[31] S.C. Jung, Y.-K. Han, Phys. Chem. Chem. Phys. 13 (2011) 21282–21287.